C.P. No. 1035

C.P. No. 1035

MINISTRY OF TECHNOLOGY

AERONAUT/CAL RESEARCH COUNCIL

CURRENT PAPERS

Calculation of the Response of a Transport Aircraft to Continuous Turbulence and Discrete Gusts and a Comparison with Flight Measurements

by

C. G. B. Mitchell

LONDON: HER MAJESTY'S STATIONERY OFFICE

1969

NINE SHILLINGS NET

U.D.C. 533.6.013.47 : 629.137.1 : 551.551 : 533.6.048.5

C.P. No.1035*
April 1968

CALCULATION OF THE RESPONSE OF A TRANSPORT AIRCRAFT TO CONTINUOUS TURBULENCE AND DISCRETE GUSTSANDA COMPARISON WITH FLIGHT MEASUREMENTS

by

C. G. B. Mitchell

SUMMARY

The symmetric response of a tri-jet transport aircraft to continuous atmospheric turbulence and to discrete ramp gusts has been calculated end compared with the results of flight measurements. The aircraft was represented by two rigid end six elastic modes, and a lifting surface theory was used to calculate airforces. Cockpit and wingtip rms accelerations relative to the cg acceleration were overestimated by the calculations, but wing end tailplane rms bending moments per g agreed with measurements to better than 12% accuracy.

---

* Replaces R.A.E. Technical Report 68083 - A.R.C.30407.

CONTENTS

1 INTRODUCTION

In the spring of 1966 a specially instrumented HS 121 Trident 1 was flown in turbulence and continuous recordings made of a number of structural accelerations and bending strains'. These recordings were analysed by Hawker Siddeley Aviation Ltd. to pmvide the spectral density, rms and number of zero crossings (N_o) for each of the response quantities over a frequency range of 0 Hz (c/s) to 12 Hz. This frequency range included, for symmetric motion, the short period oscillation and four elastic modes.

This Report describes calculations of the symmetric response of the Trident 1to continuous atmospheric turbulence, and compares the calculated and measured values of both accelerations and loads. The aircraft is shown in Fig.1, and data on the aircraft and flight condition are given in Table 1. The positions of transducers that responded to symmetric motion and whose outputs were selected for analysis are shown in Fig.2. The calculations included the pitch end heave rigid body modes, and the first six calculated elastic normal modes, which had natural frequencies between 2.8 Hz and 15.5 Hz. Because the gust input was not measured, a spectrum shape for atmospheric turbulence has had to be assumed, and it has not been possible to compare absolute values of the measured response quantities with the calculated values.

There are relatively few published comparisons of this type. Ref.2 describes the comparison of symmetric accelerations and wing loads on a swept-wing bomber for the frequency range 0 Hz to 2 Hz, which included the short period mode and the first elastic mode. Ref.3 describes the comparison of both symmetric and antisymmetric accelerations on a fighter aircraft over the frequency range 0.45 Hz to 30 Hz, which included eight elastic modes. Other unpublished comparisons have been made for a number of aircraft, including the Trident, by their respectıve manufacturers.

This present Report extends the calculation of loads to higher frequencies than Ref.2, and includes the calculation of a tail load as well as wing loads. Calculations are also made for the response to discrete ramp gusts, to determine how this compares with the response to continuous turbulence.

2 CALCULATION OF THE RESPONSE TO TURBULENCE

The method used to calculate the response of the aircraft to symmetric turbulence was similar to that of Ref.3. The equation of motion was derived from Lagrange's equation, and the axes used were those of most flutter

calculations. The origin of the axes coincides with the wing apex of the undisturbed aircraft and the axes translate without rotation along the undisturbed flight path at the steady flight speed. The aircraft was treated as a linear system, all displacements were assumed small, and the forward speed was assumed constant. Structural loads were calculated by summing the separate contributions from the airforces and inertia loads, as is described in Ref.4.

The infinity of degrees of freedom of the aircraft was approximately represented in the calculation by the rigid body modes heave and pitch, and the first six elastic normal modes calculated for the appropriate aircraft weight and cg position. The elastic mode shapes are shown in Fig.4; it was assumed that the structural damping in each mode was 0.02 of critical. It is believed that sufficient modes have been included to represent adequately both static and dynamic aeroelastic effects in the frequency range 0 Hz to 12 Hz, with the exception of resonances of the control surfaces against their jacks. The controls were taken to be fixed and control movements due to the autopilot were not included in the analysis. The autostabiliser consists of yaw and roll dampers and so did not influence the symmetric motion of the aircraft.

Davies lifting surface theory was used to calculate the airforces on the wing end tail[5]. The airforces were calculated at six frequencies on the two surfaces separately, and were added after the tailplane airforces due to the heave and pitch modes had been multiplied by $(1 - \partial\varepsilon/\partial\alpha)$ to allow for downwash from the wing modifying the flow at the tailplane. No allowance was made for the time taken for the downwash to convect from the wing to the tail.

The summed airforces at zero frequency were compared with wind tunnel measurements of the total lift and moment on the aircraft, both tail on and tail off, to assess the airforces due to the fuselage. It was found that the fuselage did not increase the lift curve slope but did move the aerodynamic centre forward by 0.11 smc (standard mean chord), and the calculated pitching moment on the aircraft was modified to fit the tunnel results. The calculated airforces due to the gust included penetration effects but did not allow for any variation of the gust velocity across the span of the aircraft.

The lifting surface computer programme used to calculate the airforces did not automatically yield the bending moments on the wing and tail. Therefore a special procedure was needed to find the aerodynamic contributions to these moments. This was done by including in the airforce calculations

synthetic modes that had displacements that were zero inboard of the line about which the moment acted, and increased linearly with distance normal to the line outboard from it. Because the computer programme uses polynomials to fit the mode shapes these synthetic modes, which contain discontinuities of slope, are not well represented in the calculation. In particular, over the inner portion of the wing where the modal displacements should be uniformly zero they are not. because of the waviness of the polynomial approximations to the modes. Thus when, in the calculation of the generalised forces, the integral over the whole wing of the product of the local pressure and displacement is evaluated it will contain an unwanted contribution from the inner wing. This will cause errors in the calculated generalised forces, particularly for moments at the more outboard stations.

The equation of motion for the modal response of the aircraft to continuous harmonic gusts was solved at approximately eighty values of the frequency parameter, and from these solutions the transfer functions for structural accelerations and loads derived. The spectral densities of the responses to continuous atmospheric turbulence were calculated assuming that the turbulence had a spectral density $\Phi_{ww}(\Omega)$ given by

$$\Phi_{ww}(\Omega) = \frac{L}{\pi} \frac{1 + 8/3\ (1.339\ L\ \Omega)^2}{[1 + (1.339\ L\ \Omega)^2]^{11/6}} \qquad (1)$$

where Ω is the wave number in rad/ft, and L is the scale length, which in this calculation was chosen as 2500 ft (762 m). Further calculations were also made in which L was varied from 250 ft (76 m) to 5000 ft (1525 m). Spectra of various scale lengths are shown in Fig.5.

In addition to the spectral densities the values of the response rms, N_o, and "dynamic response factor" (defined as response rms/rms of the structural acceleration near the cg) were calculated for comparison with the flight measurements. The response rms for unit rms excitation is given the symbol A, so the dynamic response factor can be defined as $A_{local}/A_{cg\ structural}$ for accelerations and $A_{load}/A_{cg\ structural\ acceleration}$ for loads. A and N_o were obtained from the calculated spectral densities by integration over the frequency range 0.2 Hz to 12 Hz, assuming that the response and its first derivative were Independently random and had Gaussian pmbability distributions.

Because the measurements of wing bending moments in flight consisted of measuring the ratio of the bending strains per g in turbulence to that in slow

manoeuvres[1], the low frequency response of the aircraft to control movements was calculated, and the results of this calculation used to predict the ratio of wing loads in gusts and manoeuvres. The tailplane bending moment per g in turbulence was calculated directly. The ratio of rms load per rms g in turbulence to the load per g in a slow manoeuvre is called the turbulence response factor.

Finally, calculations of the response of the aircraft to step gusts and to ramp gusts of lengths between 0 ft and 300 ft (91 m) were made, using the Fourier transform method of Ref.4. These are intended to check the method for the calculation of transient loads, and to show how the dynamic and turbulence response factors for discrete gusts end continuous turbulence compare.

3 FLIGHT MEASUREMENTS

For the flight measurements a series 1 Trident (G-ARPB) was used, as is fully described in Ref.1. The aircraft was fitted with twelve accelerometers, of which seven were sensitive to symmetric motion; the positions of these in the airframe are shown in Fig.2. Strain gauges were fitted to measure bending strains at three stations on the port wing, one on the starboard wing, and at the tailplane root. All these measurements were recorded as analogue signals on magnetic tape. Other recorder channels were used for control angles, other strain gauges, aircraft speed, aircraft attitude and angular rates, end auto-pilot monitoring signals. It has been assumed that the measured bending strains were directly proportional to the bending moments, whatever the load distribution.

The tailplane bending moment strain gages were calibrated in flight by applying known tail loads through movements of the flaps and spoilers. The wing bending moment gauges were also calibrated in flight, by manoeuvres in which the normal acceleration was increased and then decreased. These manoeuvres were made at a constant Mach number and various altitudes to find the variation of wing strain per g with dynamic pressure. Thus the wing structural loads were not measured as absolute quantities, but in terms of the strains per g in manoeuvres.

The aircraft was flown in turbulence on three flights. The measurements analysed were those made during runs 18, 19 and 20 of flight 738 (see Ref.1). All these runs were at approximately 15300 ft (4663 m) altitude and 268 kt (497 km/hr) eas. For run 18 the autopilot and dampers were engaged, for run 19 the dampers were engaged, and for run 20 neither the autopilot nor the

dampers were in use. The autopilot and dampers can be expected to modify the response of the aircraft at frequencies below 2 Hz.

For spectral analysis the measurements were digitised at 100 points per second and filtered digitally to reduce the effect of drift during digitising. This filter had a time constant of 3.2 seconds. For runs 18 and 20 the sample length was 35 seconds, while for run 19 it was 55 seconds. Spectra were calculated digitally through the autocorrelation function, using a maximum lag of 5 seconds. All values of the response rms and N_o quoted in this Report are obtained by integration of these spectra over the frequency range 0.2 Hz to 12 Hz. In Ref.1 the rms were obtained by the direct summation of the squares of the measurements, digitised at 5 points per second. Because of this the values of rms and N_o given here and in Ref.1 do differ by a few per cent.

To increase the statistical reliability of the measured spectra the author of this Report has averaged the spectral densities from runs 18, 19 and 20 for frequencies greater than 2.0 Hz, giving the spectra from each run equal weight. Below 2.0 Hz the spectra may be modified by the action of the auto-pilot, and possibly also the dampers, and the spectra from run 20 alone are used for comparison with the calculation. The spectra that result from this process were then smoothed by eye, ripples less than ±25% of the local spectral density being considered insignificant. The smoothed and unsmoothed spectra were made to coincide at major peaks and troughs.

4 RESULTS

Figs.5 and 6 show the calculated and measured spectra for structural accelerations. These are for symmetric motion only, with the exception of the measured spectrum for the tailplane tip acceleration, which contains both symmetric and antisymmetric motion. The calculated spectra are for a 1 ft/s tas (0.305 m/s) gust velocity, while the measured are for an unknown gust velocity, which can be deduced to have been about 7.5 ft/s (2.3 m/s) tas. This velocity has been derived by comparing the power at the short period peak of the measured and calculated responses, assuming the excitation spectrum has a scale length of 2500 ft (762 m). In Fig.5 the variation in height of the short period peak at 0.4 Hz with fore-end-aft position on the aircraft can be clearly seen. The variation is greater for the measured spectra than for the calculated spectra, showing that the aircraft pitches more at the short period frequency than the calculation predicts.

Fig.7 shows the calculated and measured spectra for wing bending moments, expressed in terms of the equivalent acceleration at the centre of gravity during a slov manoeuvre. It will be noticed that the experimental short period peak for the moment at rib 13 is not as high as the peaks for the moments at the wing root and at rib 8. The peak at 10.2 Hz on the experimental results is attributed by gawker Siddeley Aviation Ltd. to a mode involving predominantly symmetric rotation of the elevators.

Fig.8 shows the calculated and measured spectra for the bending moment at the tailplane root. Fig.9 plots the variation with position on the wing of the turbulence response factor and N_o for the wing bending moment. It can be seen that the calculation predicts a greater high frequency content at the outboard stations then occurs in practice.

Fig.10 shows how the overall rms and N_o of the accelerations at the cockpit, the structure near the cg, and the wingtip increase as the upper cut-off frequency for integration of the spectra is raised. Fig.11 shows how these same rms vary if the scale length of the turbulence exciting the aircraft, L in equation (I), ranges from 250 ft (76 m) to 5000 ft (1525 m). The integration frequency range for Fig.11 is 0 Hz to 12 Hz.

Table 2 lists the calculated values of A end N_o for all the response quantities, for excitation by turbulence with a scale length of 2500 ft (762 m). Table 3 gives the calculated wing bending moments in a slow manoeuvre . Tables 4 and 5 compare the calculated end measured values of the dynamic and turbulence response factors and N_o for all the response quentities. Results from runs 19 and 20 are given to show the scatter between runs, on the assumption that the dampers did not affect the rms of the symmetric response quantities.

Fig.12 shows the calculated transient response of the aircraft to a 1 ft/s (0.305 m/s) step gust. From this the response to discrete gusts of any shape can be synthesised by superposition. In Fig.13 are given the peek responses to ramp gusts with a range of ramp lengths, and the variation with gust ramp length of the wing end tail bending moments per unit acceleration of the structure near the cg. It will be seen that the load per g is not very sensitive to the gust ramp length.

5 DISCUSSION

The measurements show that the aircraft pitches about 10% less at the short period frequency then is predicted by the calculation. Also, the

measured dynamic response factors for accelerations at the cockpit and wingtip are less than the calculated factors, indicating that, in addition to the pitching discrepancy, the aircraft does not vibrate structurally as much as the calculation would suggest. This latter result is similar to the results of Ref.3, although on the fighter aircraft of that study the effect was even more marked.

The turbulence response factors for the wing bending moments (Fig.9) agree with the measurements to within 10% at the root, 12% at rib 8, and 6% at rib 13, but the calculated and measured trends along the wing are rather different. The calculated tailplane root bending moment agrees with the measured moment per g to 9%. The calculated and measured N_o agree reasonably well, the largest difference occurring in the results for the tailplane root bending moment, where the measured N_0 is 18% to 35% larger than the calculated value. However, since the elastic modes contribute only slightly to the structural loads, this aircraft does not provide a very rigorous test of the calculation.

The turbulence response factors for the wing bending moments reflect at least two effects. The first of these is that in turbulence the wing vibrates at the frequency of the structural modes, and that for a given wing lift this generally increases the bending moment relative to that in a slow manoeuvre. The second is that, at the forward cg positron used for the flight tests, in a manoeuvre the incremental tail load to cause a positive Incremental normal acceleration is downwards and is equal to 7% of the Incremental wing lift, while on entering an up gust the tall load is upwards and is equal to 12% of the wing lift. Therefore some 20% more wing lift is required to cause a given normal acceleration Increment in a manoeuvre than in a gust. correspondingly, the turbulence response factor for wing bending moments, in the absence of structural vibration, would be about 0.83.

The shapes of the calculated and measured response spectra agree well, except that the calculated structural resonance frequencies are a little lower (about 10%) than the measured frequencies, and some discrepancies occur at the higher frequencies. The modes used for the calculation were calculated, and may have been based on stiffnesses a little lower than were achieved in practice.

The calculations of the response to discrete ramp gusts predict that the structural loads per unit acceleration of the structure near the cg do not vary much with gust ramp length. These calculations lead to response factors for wing loads that are larger than the factors from the spectral calculations by 1% to 5%, and which differ from the measured factors by 7% to 14%. The tailplane root bending moment calculated for discrete gusts is some 17% lower than that calculated for continuous turbulence, and 7% lower than the measured moment.

The quality of agreement noted here occurs when the calculations are compared with the quantities that were measured directly. On the wing the agreement for the turbulence response factors is better than that for the bending moments per g themselves, probably because the calculated airforce contributions to the moments are not very accurate, particularly at the more outboard stations.

The calculations described in this Report have been made using only information that would be available at the design stage of an aircraft. The results suggest that this standard of calculation overestimates the contribution of the elastic modes to the accelerations at the extremities of the aircraft by perhaps 20%, but that the turbulence response factors for the major structural loads can be calculated to an accuracy that is approaching that required for design purposes. It is likely that this accuracy, when the response calculations are used in conjunction with normal stressing methods to calculate the load distribution in manoeuvres, is as good as that of the flight measurements. It must be remembered, however, that the elastic modes are contributing little to the structural loads measured on this particular aircraft.

On the aircraft considered here the wing loads per unit acceleration of the structure near the cg predicted from discrete gust and continuous turbulence calculations are not appreciably different, and although the tail loads g differ by 17% the measured tail load is almost mid-way between them. The discrete gust used in this Report is of ramp form, while civil aircraft are usually designed to requirements that define a gust of (1 - cosine) shape.

The author of this Report does not believe that the calculation techniques described here are any more sophisticated than those in use in the aircraft industry, so that the results given here indicate the confidence that can be placed on such calculations.

6 CONCLUSIONS

Calculations of the response of a transport aircraft to continuous turbulence overestimate the degree of excitation of the elastic modes, but predict the tail root bending moment, and the turbulence response factors for the major wing loads, to accuracies better than 12%. Calculations of the response to discrete ramp gusts predict the tail root bending moment and the wing load response factors to the same accuracy as the spectral calculations.

The calculations described here are typical of those performed in the aircraft industry, and comparison of the calculated and measured responses of the aircraft to turbulence indicates that the accuracy of the calculation of major structural loads is approaching that required for design purposes. It is likely that the overall accuracies of the flight measurements and the calculations are similar. On the particular aircraft considered the elastic modes contributed only slightly to the structural loads.

ACKNOWLEDGEMENTS

The author wishes to thank Hawker Siddeley Aviation Ltd., Hatfield, for supplying data that made these calculations possible, and for allowing the reproduction of flight test results that were additional to those reported in Ref.1.

The author would also like to thank British European Airways for permission to use the photograph printed as Fig.1 in this Report,

Table 1

AIRCRAFT PRINCIPAL DATA

Aircraft: HSA 121 Trident series 1, G-ARPB

wing span	89.84 ft	27.38 m
length	114.75 ft	34.93 m
standard mean chord	15.13 ft	4.61 m
wing area	1358 ft^2	126.2 m^2
sweepback at $\frac{1}{4}$ chord	35"	35"

Flight 738

weight	90820 lb	41188 kg
cg position at	0.113 smc	0.113 smc
altitude	15300 ft	4663 m
speed (tas)	586 ft/sec	178 m/sec
Mach number	0.55	0.55
$\partial C_L/\partial\alpha$	4.94 per rad	4.94 per rad
$\frac{\rho V S \partial C_L/\partial\alpha}{2W}$	0.0323 g ft^{-1} sec	0.1060 g m^{-1} sec

Table 2

CALCULATED SYMMETRIC RESPONSE IN RANDOM TURBULENCE

	A		N_o Hz (c/s)
	per 1 m/sec gust	per I ft/sec gust	
accelerations (normal) centre of gravity			
structure near cg	0.0649 g	0.0193 g	1.75
cockpit	0.0590 g	0.0180 g	4.05
tailplane centreline	0.0971 g	0.0296 g	2.54
wing tip	0.3336 g	0.1017 g	4.49
tailplane tip	0.2201 g	0.0671 g	7.41
bending moments			
wing root rib	34930 Nm	7850 lb ft	1.34
wing rib 8	15600 Nm	3505 lb ft	1.53
wing rib 13	3290 Nm	739 lb ft	1.96
tailplane root	2034 Nm	457 lb ft	1.90

Table 3

CALCULATED RESPONSE TO A SLOW HARMONIC ELEVATOR MOVEMENT

	bending moment Nm/g	bending moment lb ft/g
wing root	616970	455000
rib 8	264419	195000
rib 13	53965	39800

Table 4

CALCULATED AND MEASURED DYNAMIC AND TURBULENCE RESPONSE FACTORS

	calculated	measured (run 19)	measured (run 20)
accelerations			
cockpit*	0.91	0.70	0.77
tailplane centreline*	1.50	1.50	1.52
wing tip*	5.14	5.07	4.10
tailplane tip*	3.39	3.47[x]	4.03[x]
bending moments			
wing root rib**	0.87	0.96	0.95
wing rib 8**	0.91	1.03	1.01
wing rib 13**	0.93	0.87	0.89
tailplane root †	23100 lb ft/g (31310 Nm/g)	21300 lb ft/g (28880 Nm/g)	21200 lb ft/g (28743 Nm/g)

*dynamic response factor defined as $A_{local}/A_{structure\ near\ cg}$

**turbulence response factor defined as $\frac{A_{moment}/A_{structure\ near\ cg}}{\text{moment g due to manoeuvre}}$

†dynamic response factor defined as $A_{moment}/A_{structure\ near\ cg}$

[x] includes antisymmetric motion

Table 5

CALCULATED AND MEASURED FREQUENCIES OF ZERO CROSSINGS

	calculated, Hz	measured (run 19)	measured (run 20)
accelerations			
structure near cg	1.75	1.61	1.63
cockpit	4.05	4.08	4.45
tailplane centreline	2.54	2.80	3.20
wing tip	4.49	4.57	5.77
tailplane tip	7.41	5.83*	5.75'
bending moments			
wing root rib	1.34	1.46	1.37
wing rib 8	1.53	1.52	1.45
wing rib 13	1.96	1.65	1.71
tailplane root	1.90	2.25	2.56

*includes antisymmetric motion

SYMBOLS

A	response rms/excitation rms
L	scale length of turbulence
N_o	frequency of zero crossings
W	vertical gust velocity
α	incidence
$\Phi_{WW}(\Omega)$	spectral density of the vertical component of atmospheric turbulence
Ω	reduced frequency radians/foot
ε	downwash angle at tailplane

REFERENCES

No.	Author	Title, etc.
1		Rough air flight tests on a Trident. Hawker Siddeley Aviation Ltd. Report HSA(Hat) Aero Dspt ./5837/WL, Hatfield (1967)
2	F. V. Bennett IC. G. Pratt	Calculated responses of a large swept wing airplane to continuous turbulence with flight-test comparisons. NASA Technical Report R-69 (1960)
3	C. G. B. Mitchell	Calculation of the response of a fighter to turbulent air and a comparison with flight measurements. R.A.E. Technical Report 66275 (A.R.C.28633) (1966)
4	C. G. B. Mitchell	Computer programmes to calculate the response of flexible aircraft to gusts and control movements. A.R.C. C.P. 957 (1966)
5	D. E. Davies	Calculation of unsteady generalised air forces on a thin wing oscillating harmonically in subsonic flow. A.R.C. R. & M. 3409 (1963)

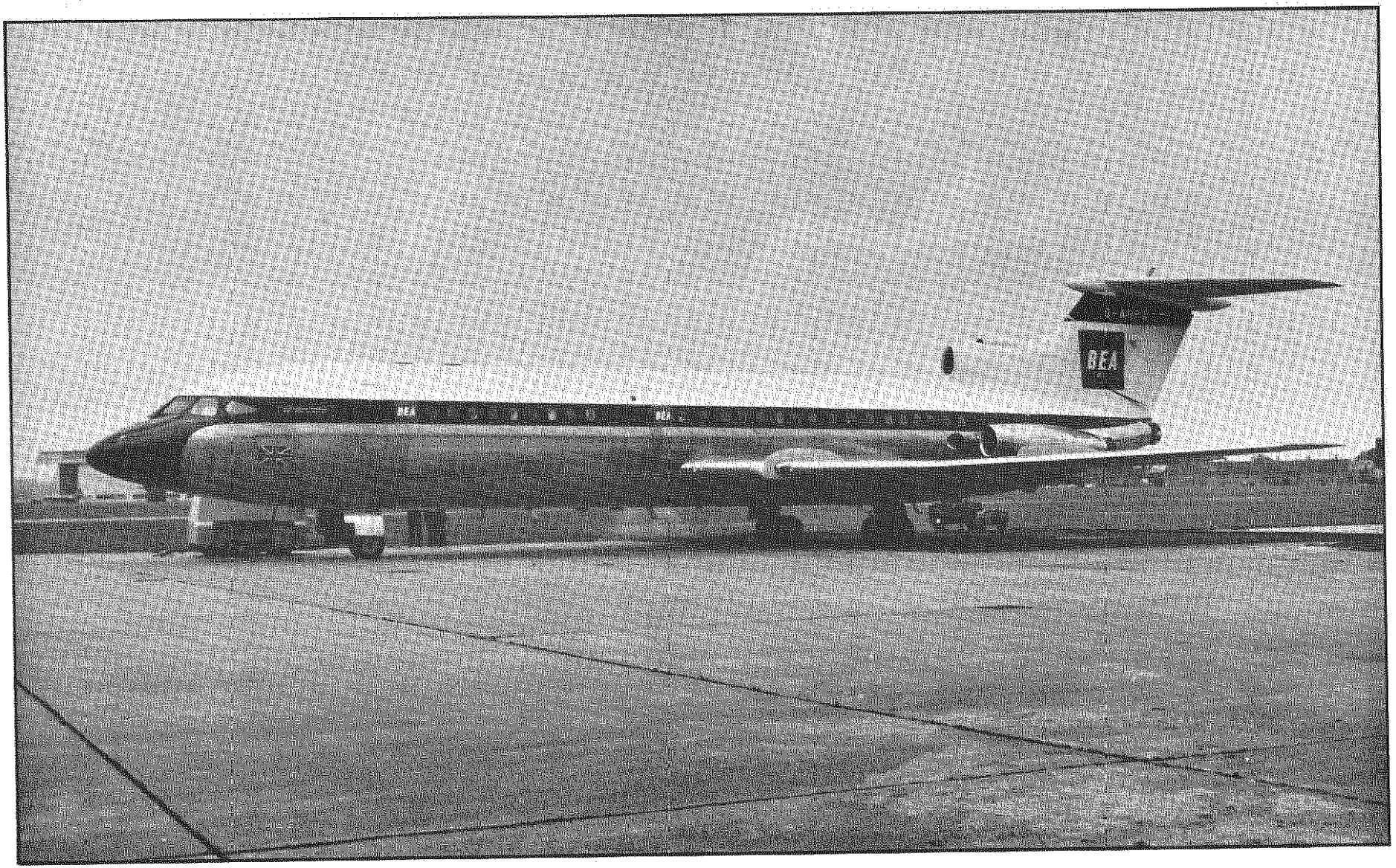

Fig.1. The est aircraft

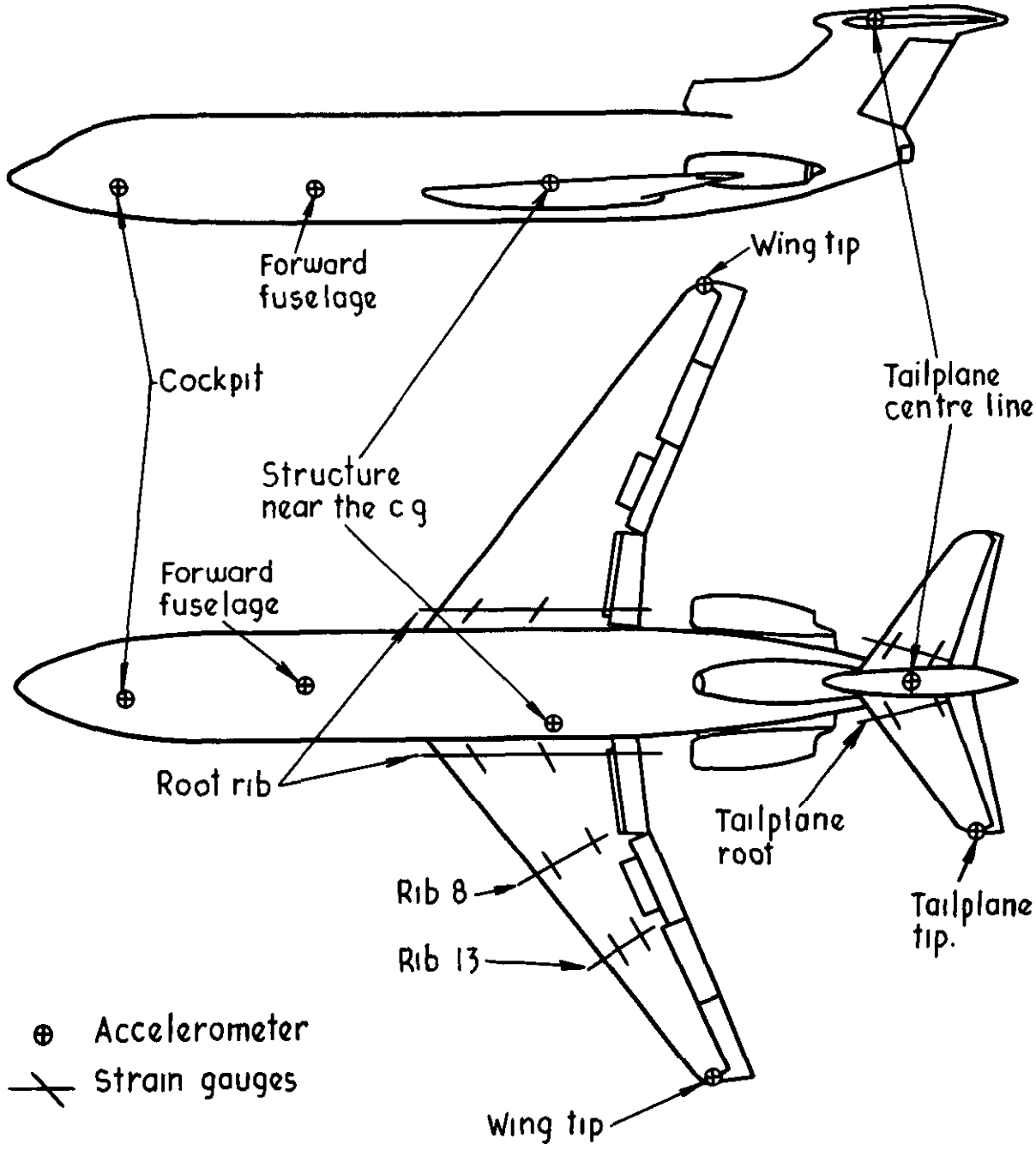

Fig. 2 Location of selected transducers.

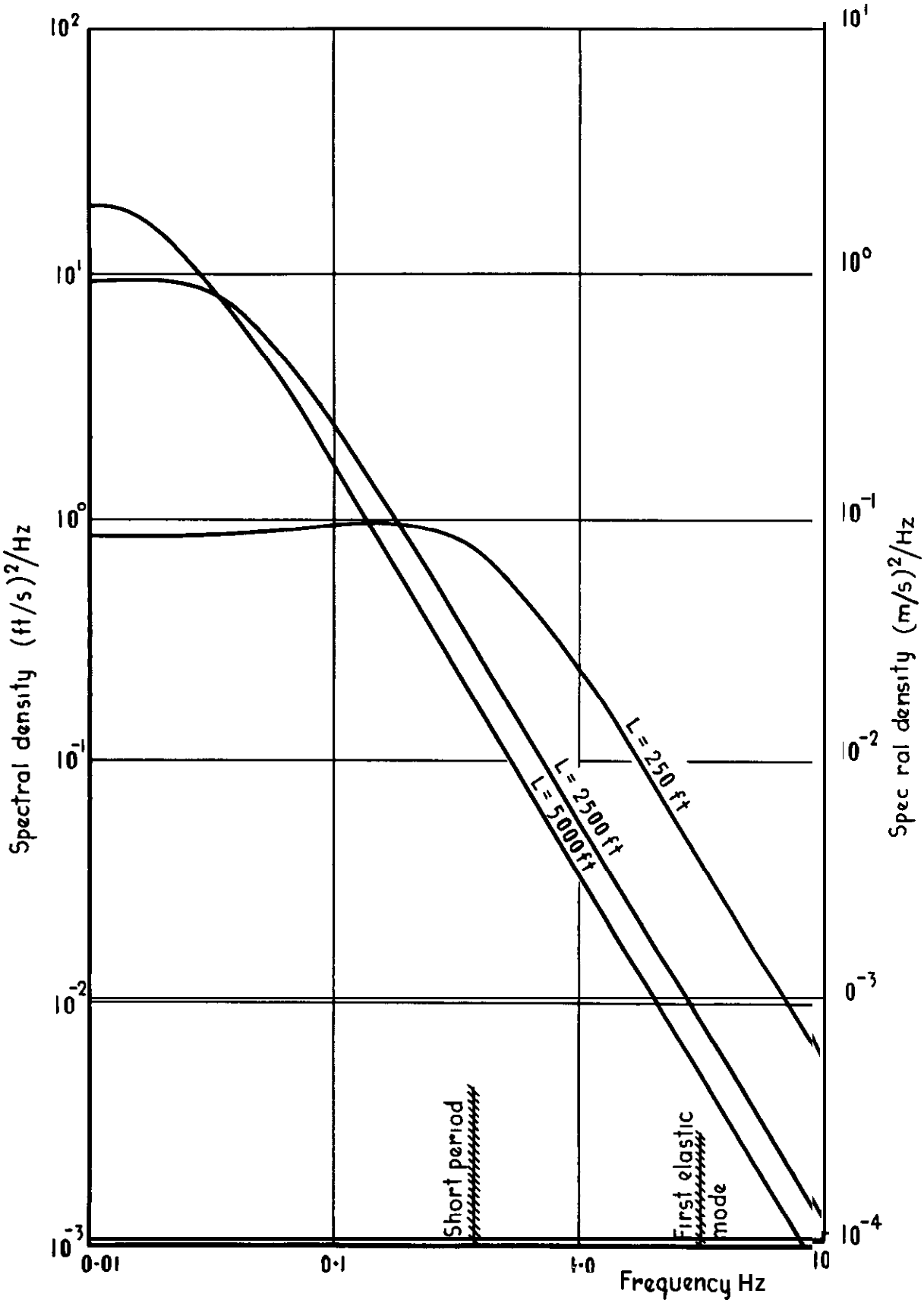

Fig.3. The von **Kármán** spectrum of turbulence for a flight speed of 586ft /sec. and unit gust velocity

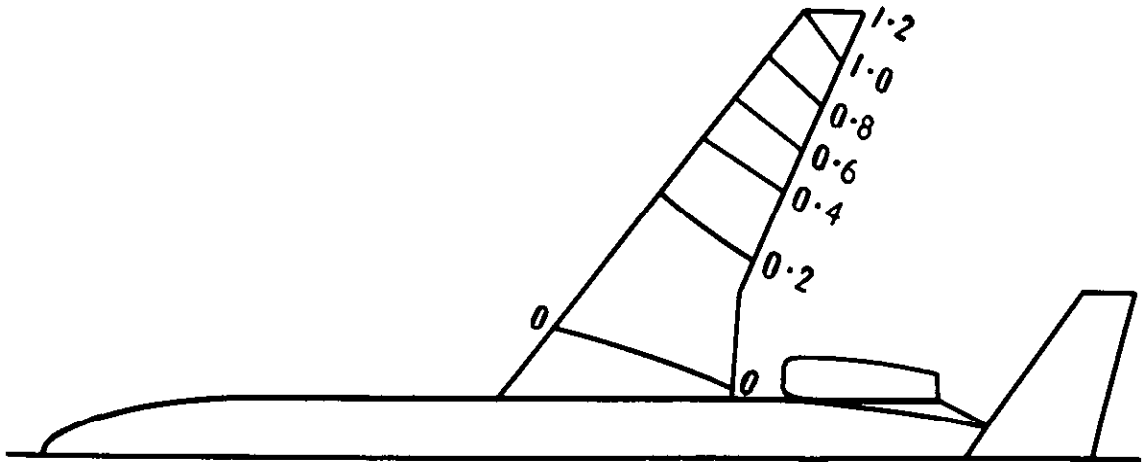

Elastic mode I 2.82 **Hz**

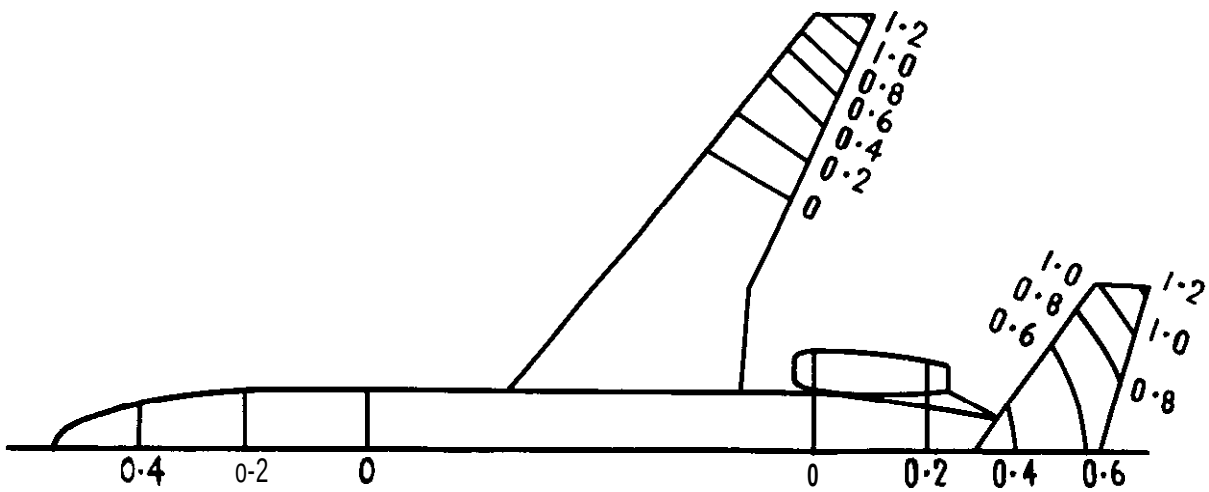

Elastic mode 2 4-85 **Hz**

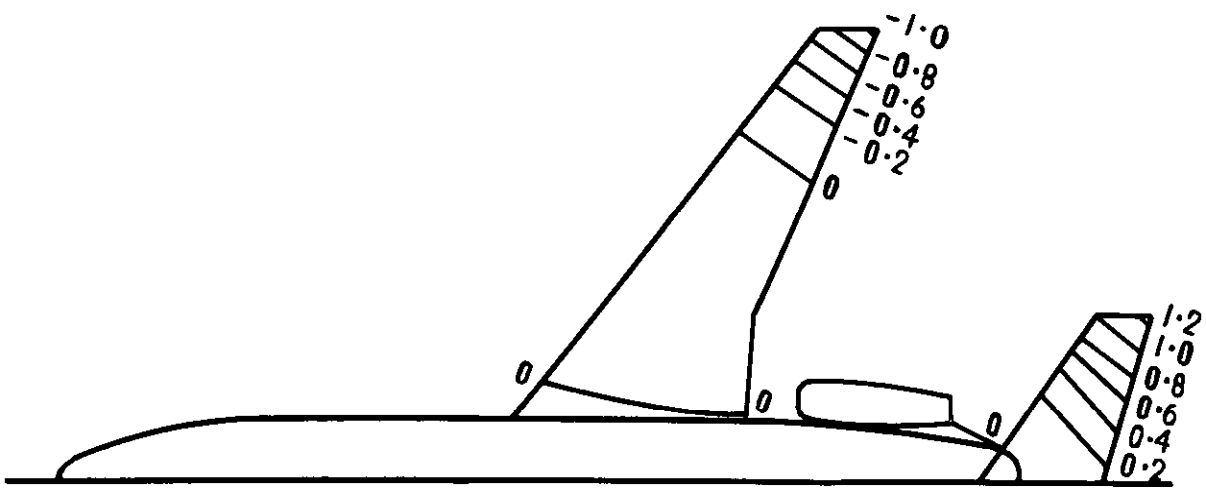

Elastic mode 3 7·69 **Hz**

Fig. 4a Calculated normal modes.

Fig 4 b

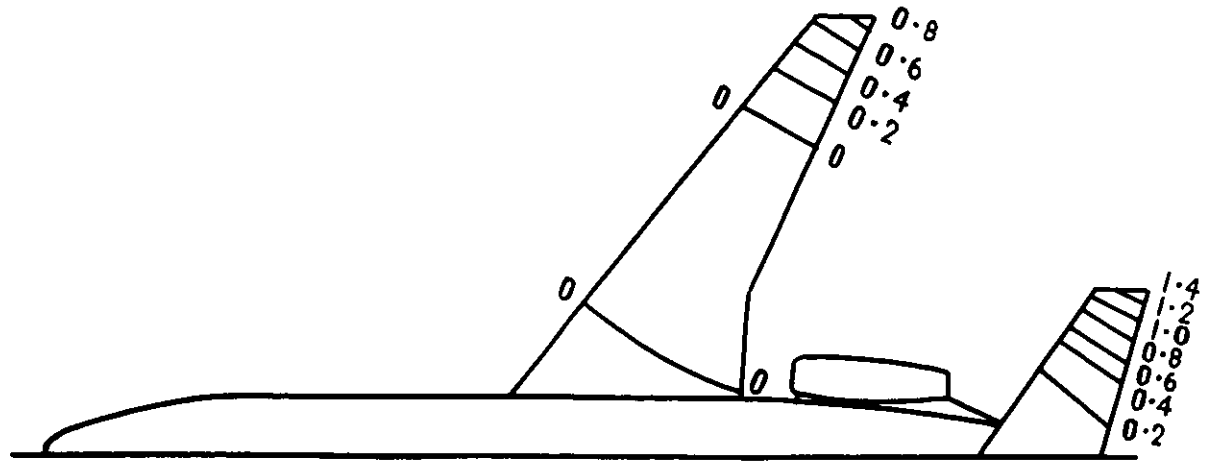

Elastic mode 4 8·10 Hz

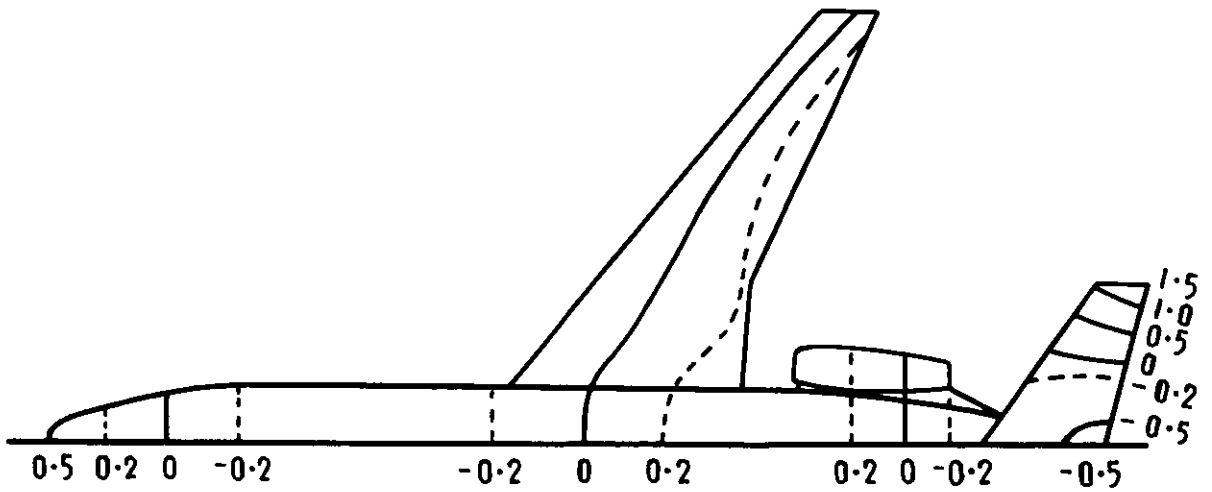

Elastic mode 5 12·9 Hz

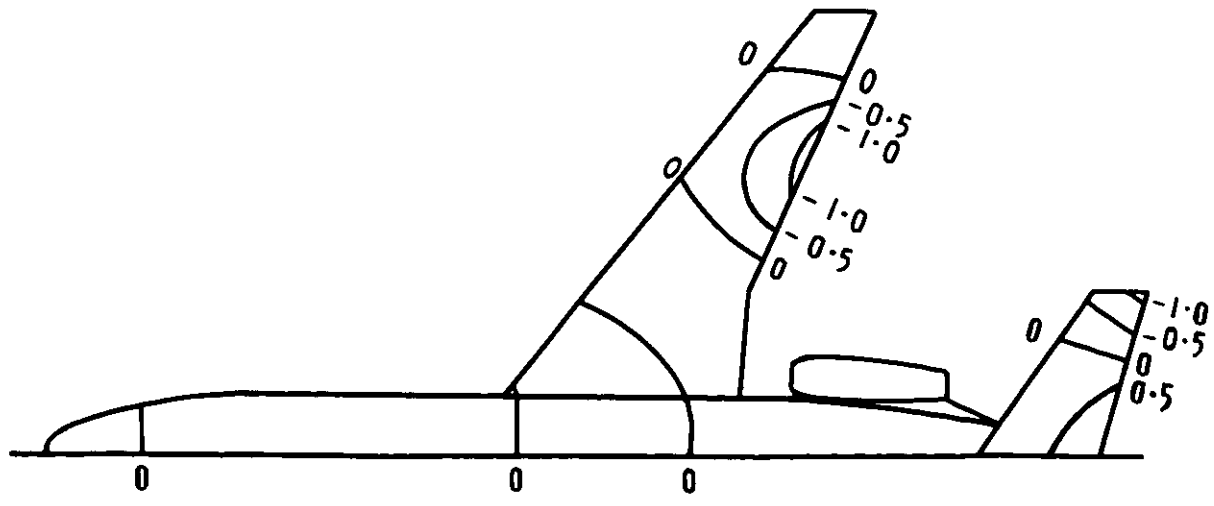

Elastic mode 6 15·5 Hz

Fig 4b Calculated normal modes.

Fig 5a&b

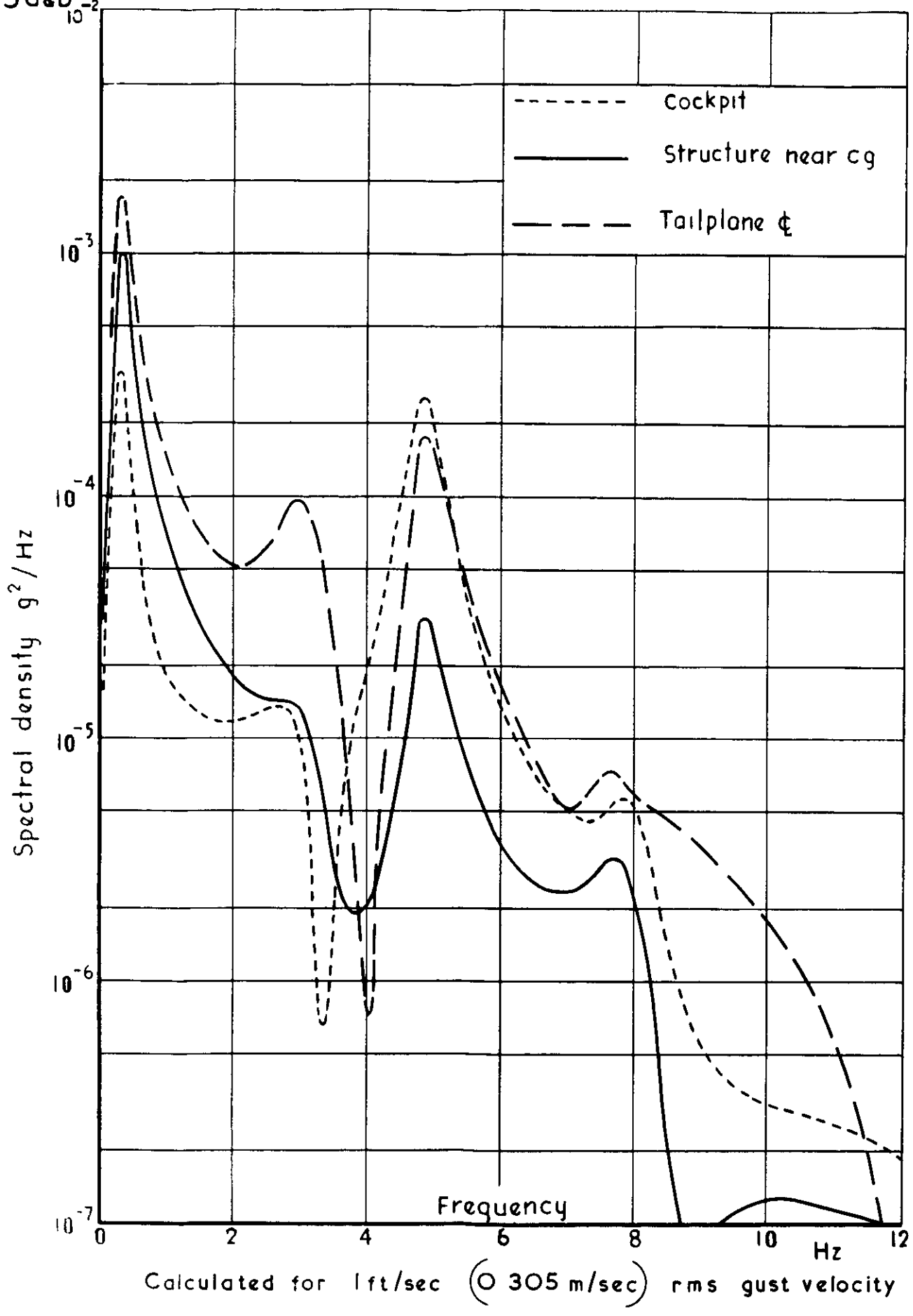

Fig 5a Calculated fuselage normal accelerations

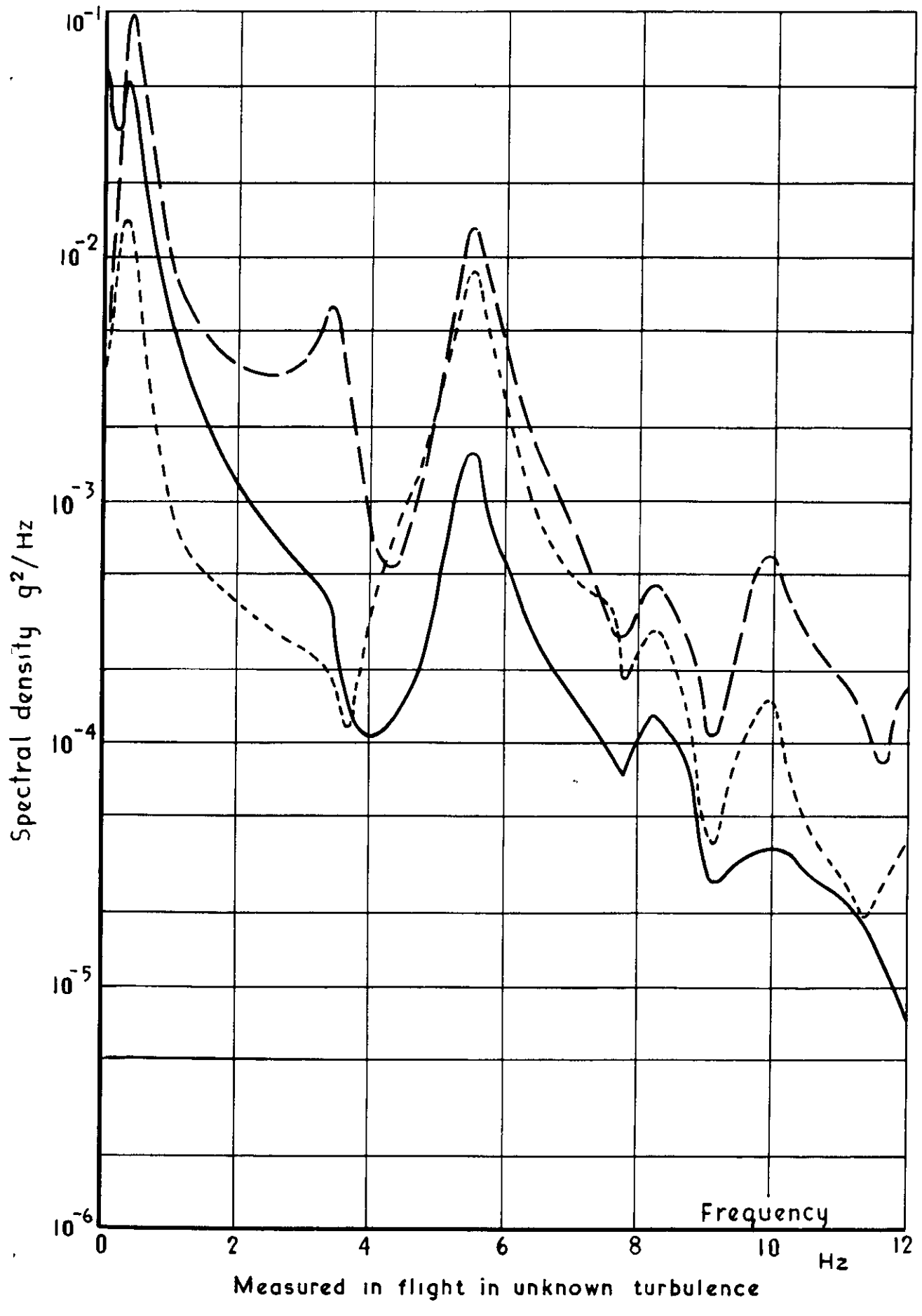

Fig. 5b Measured fuselage normal accelerations

Fig.6a&b

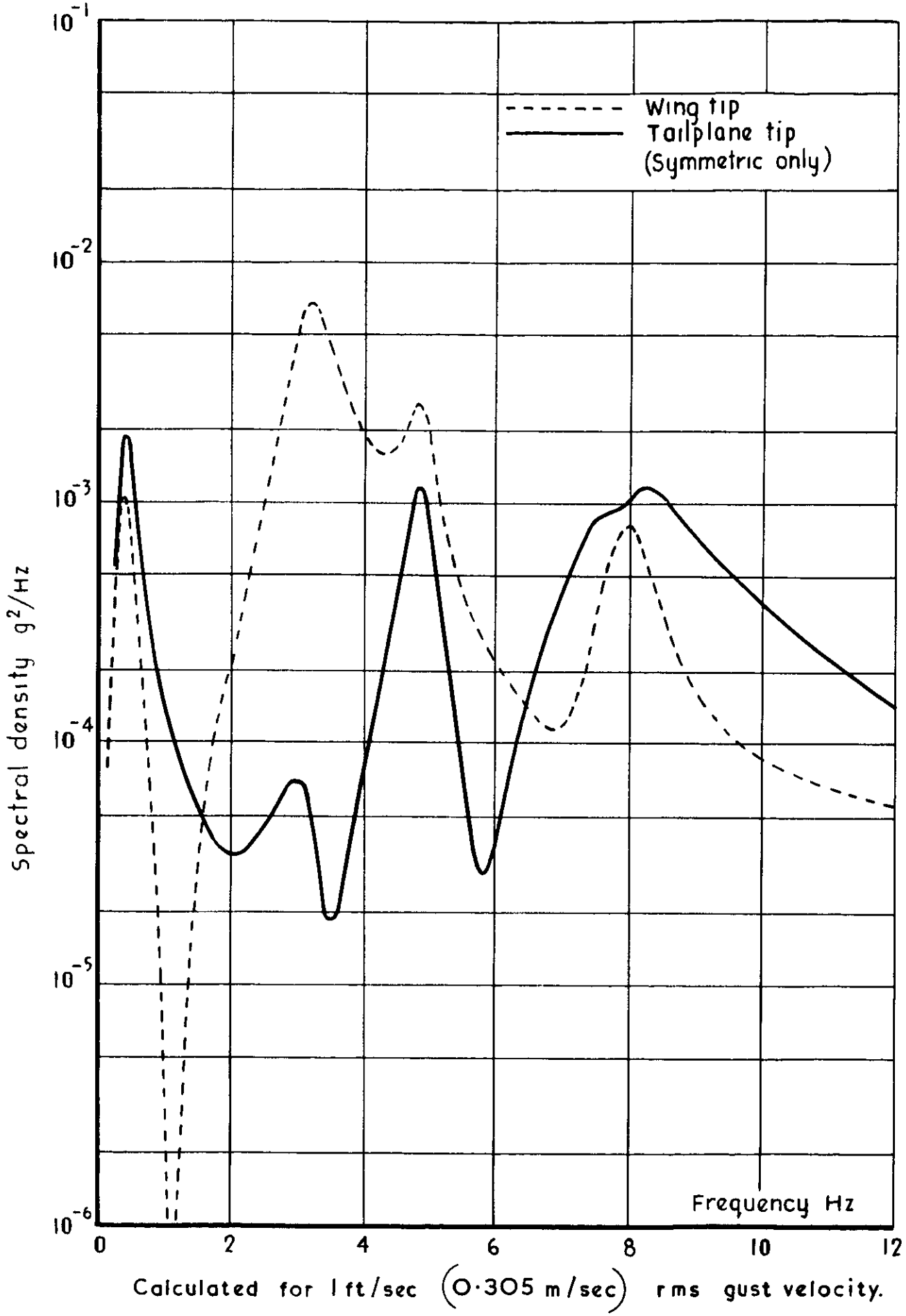

Fig 6a Calculated wing and tail tip normal accelerations.

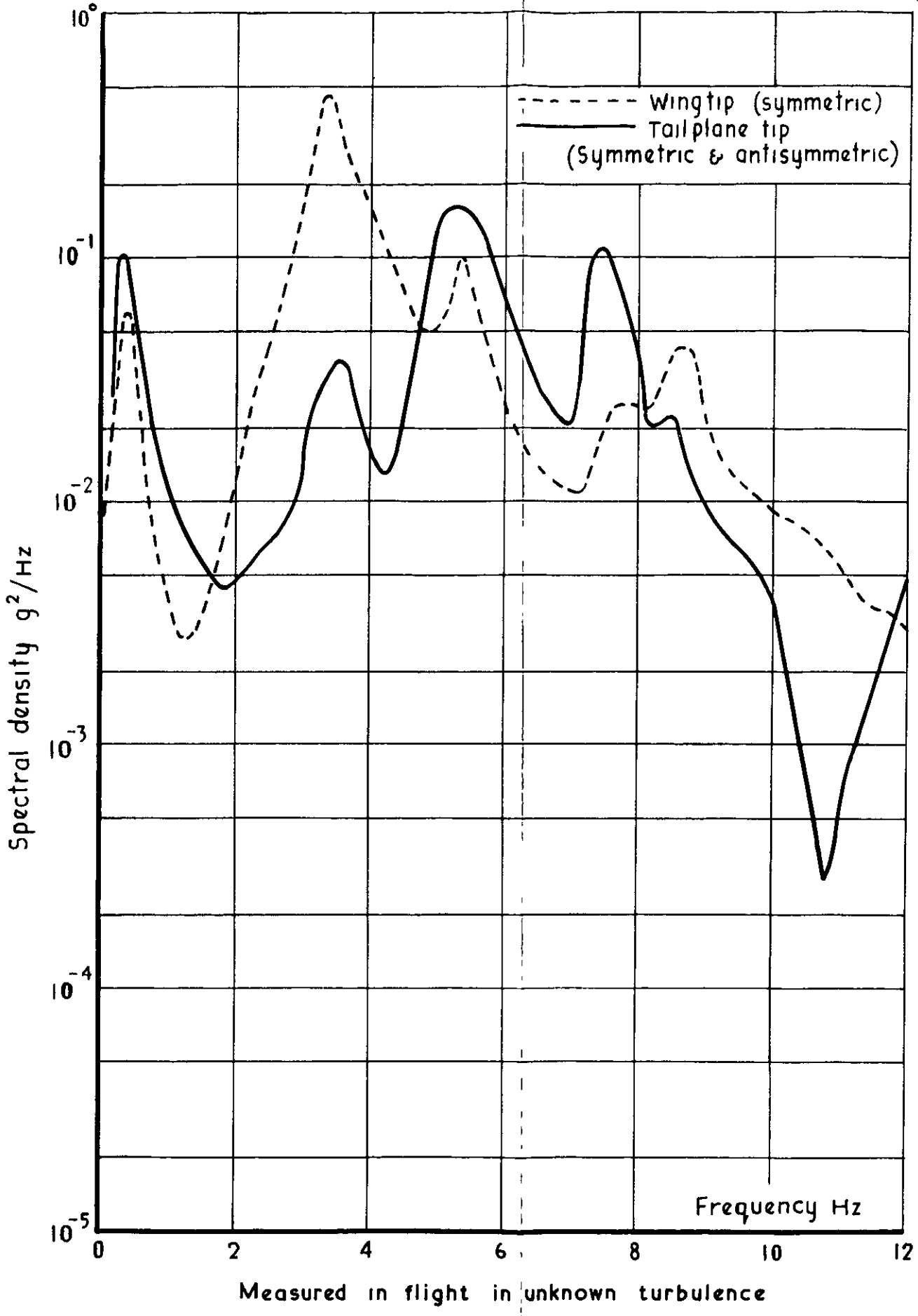

Fig 6b Measured wing and tail tip normal accelerations

Fig 7a&b

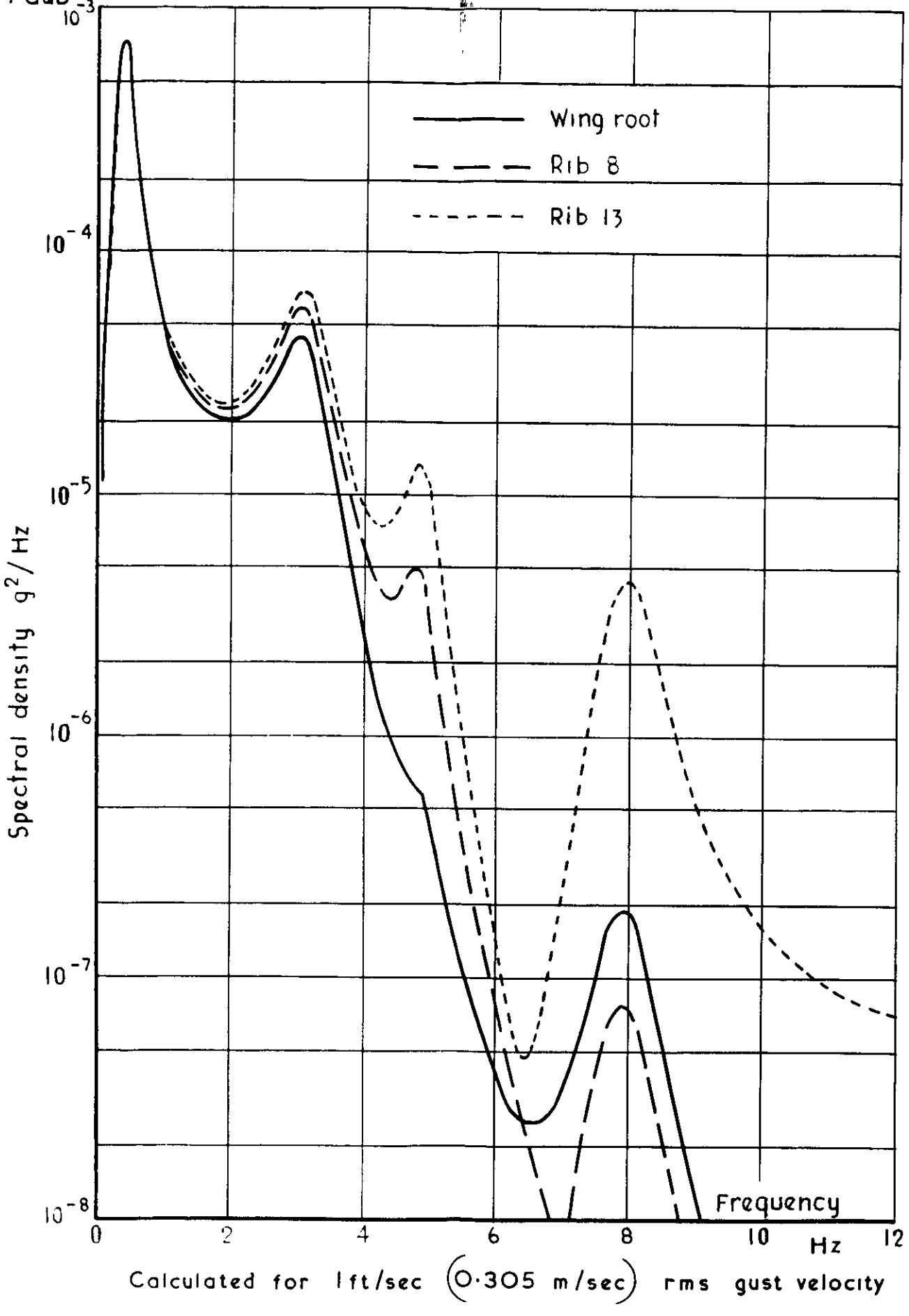

Fig 7a Calculated wing bending moments in equivalent g units

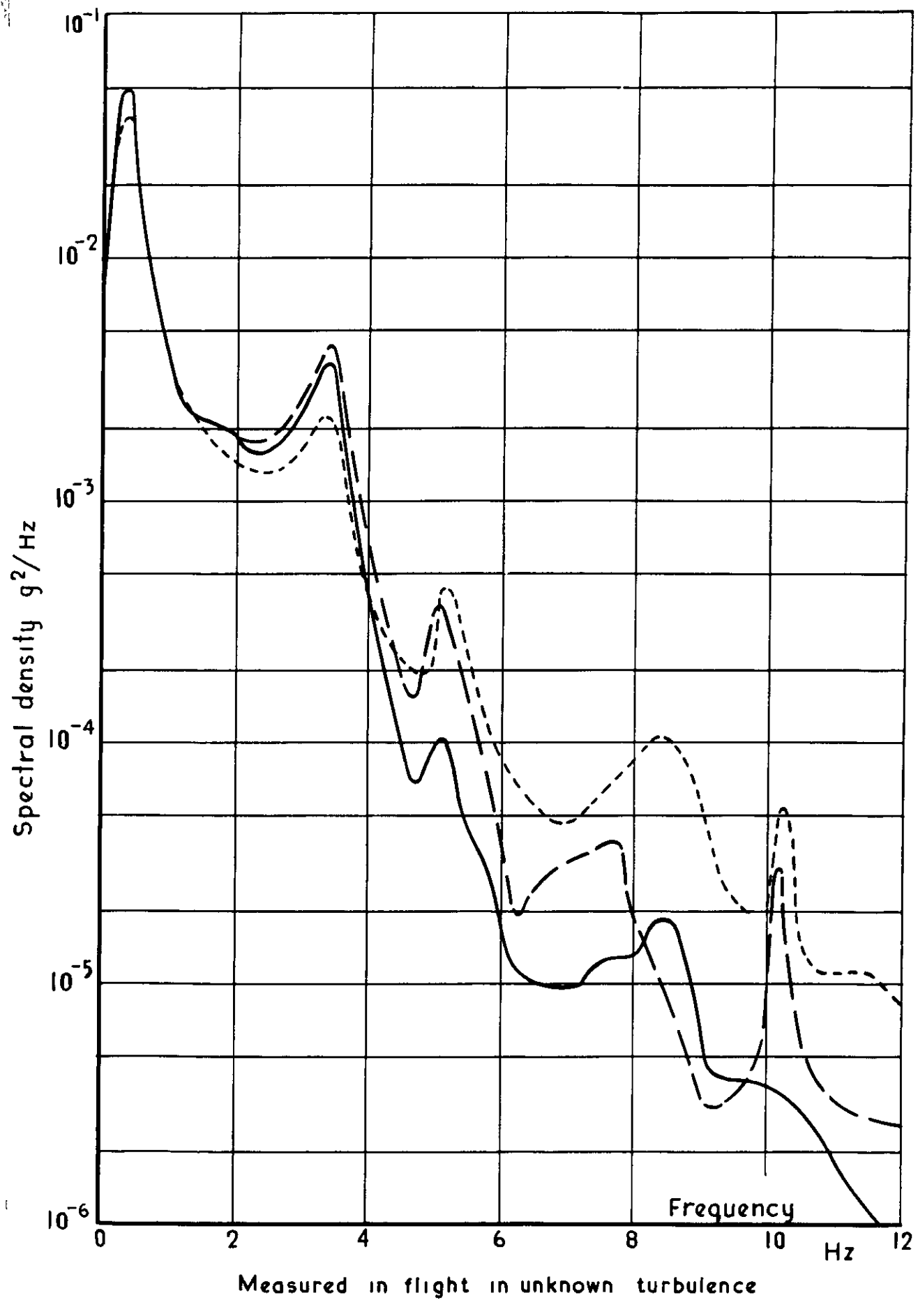

Fig. 7b Measured wing bending moments in equivalent g units

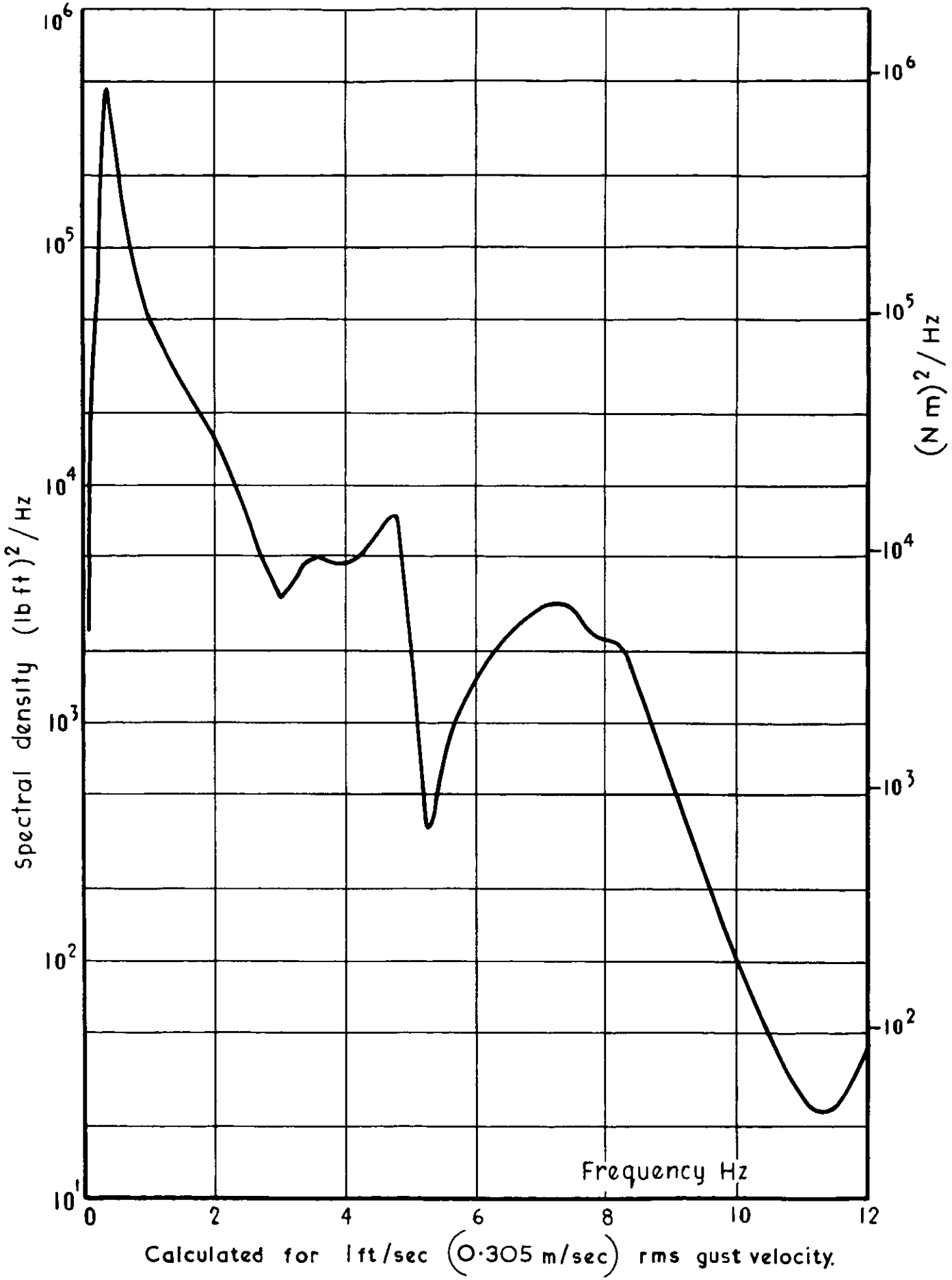

Calculated for 1 ft/sec (0·305 m/sec) rms gust velocity.

Fig 8a Calculated tailplane bending moment.

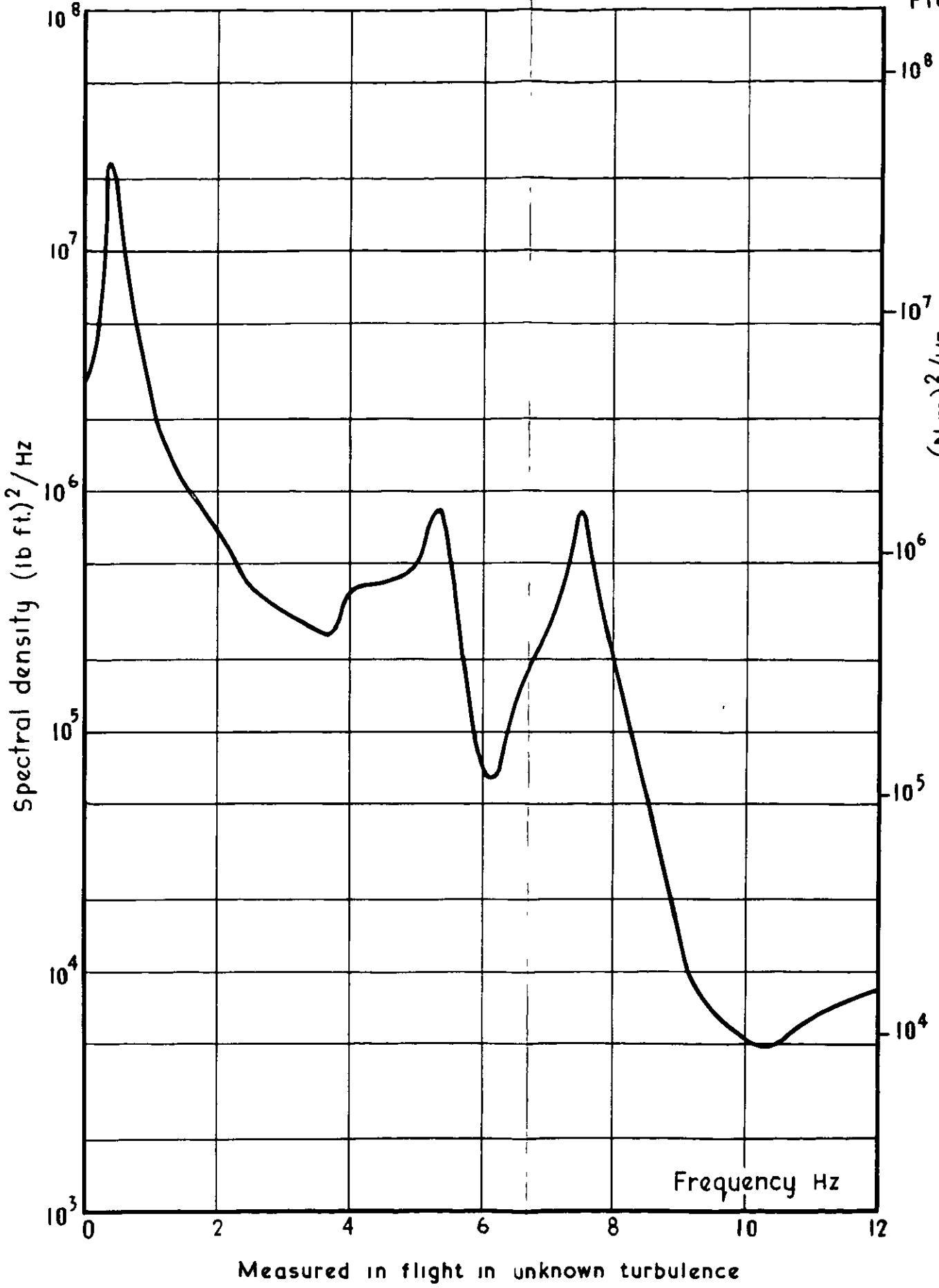

Measured in flight in unknown turbulence

Fig 8b Measured tailplane bending moment

Fig. 9

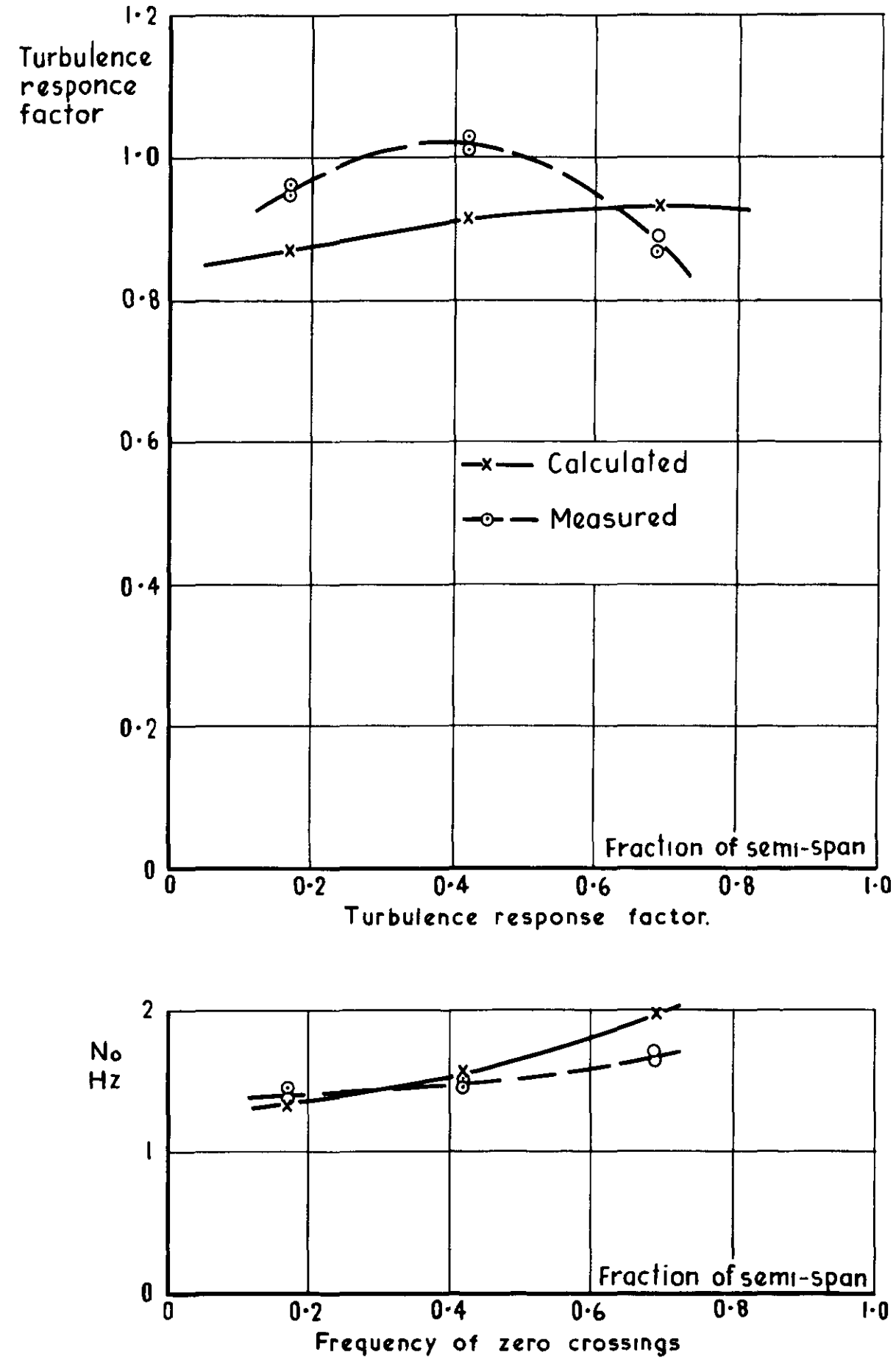

Fig. 9 Calculated and measured wing bending moments

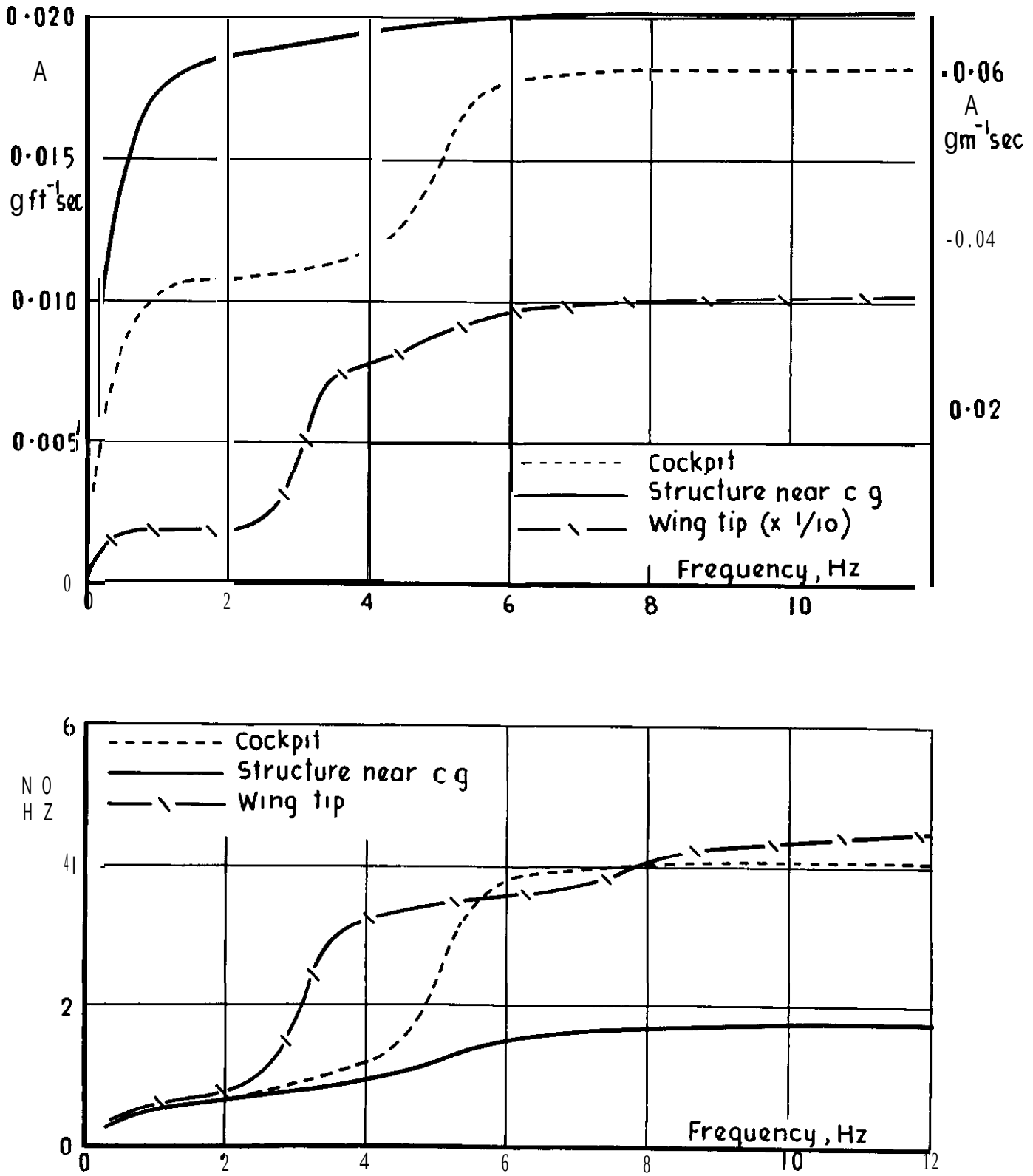

Fig. 10 Variation of A and N_o for structural accelerations with integration upper cutoff frequency.

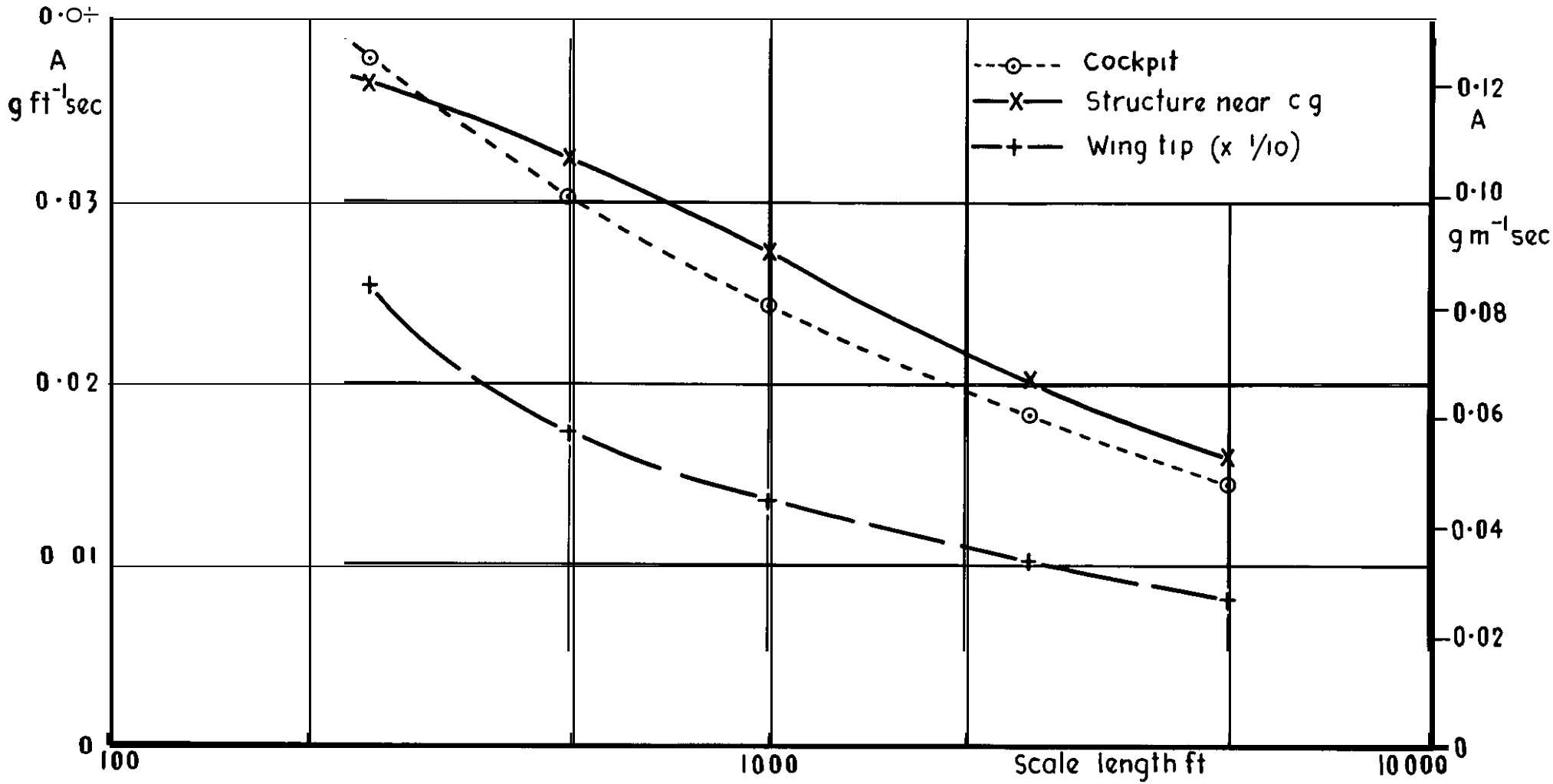

Fig. 11 Variation with turbulence scale length of A for structural accelerations.

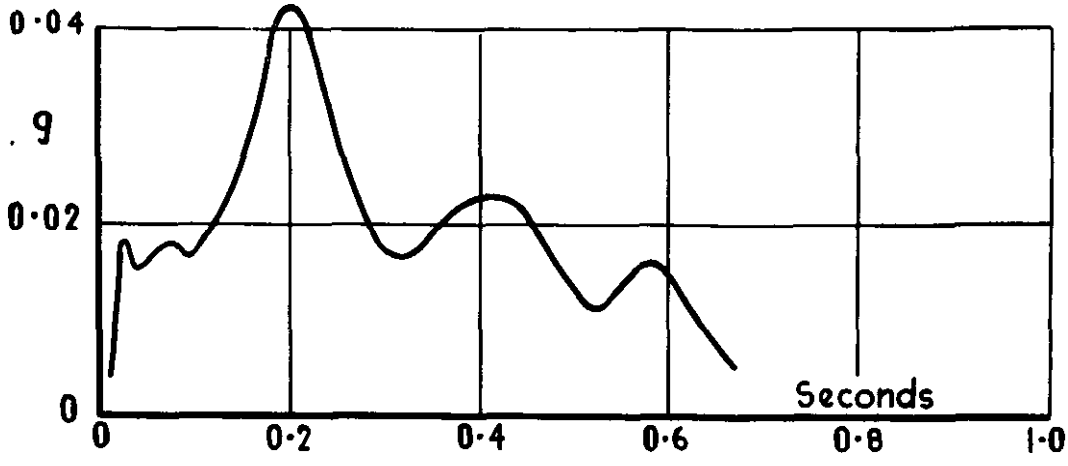

Acceleration of the structure near cq

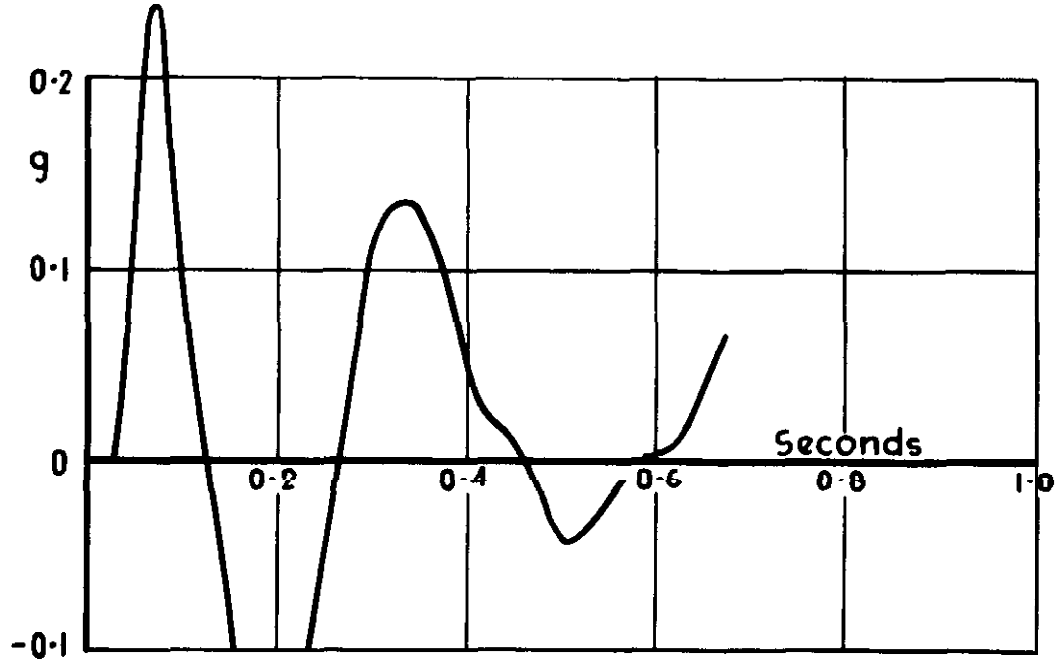

Acceleration at the wing tip.

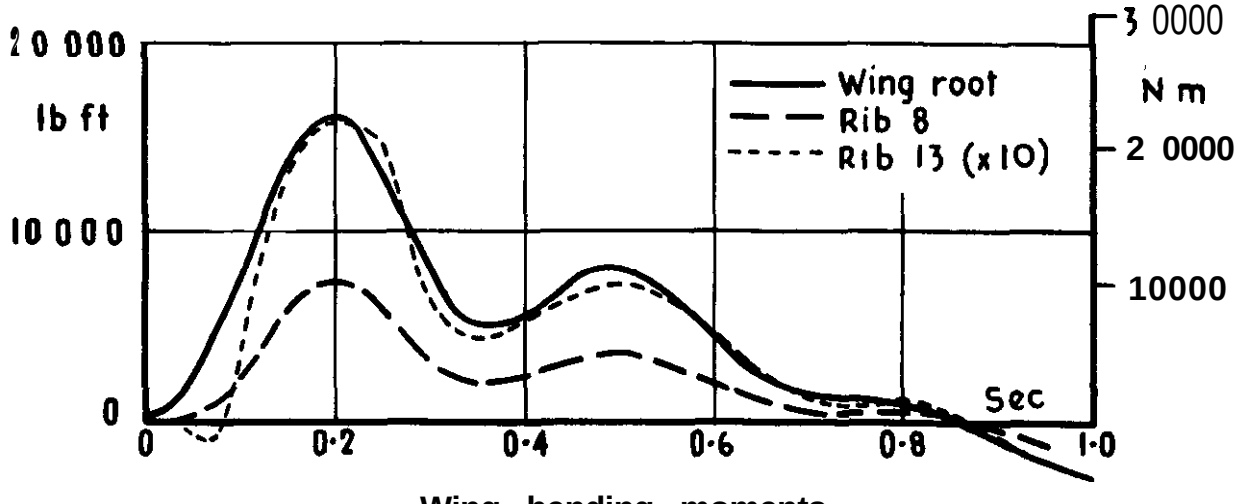

Wing bending moments

Fig.12 Transient response to a 1 ft/sec (0·305 m/sec) step gust,

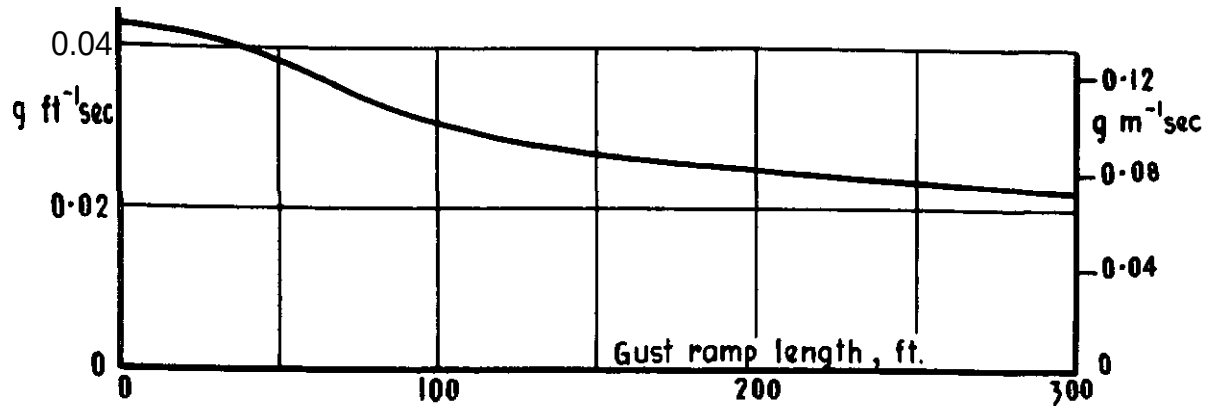

Acceleration of the structure near the cg

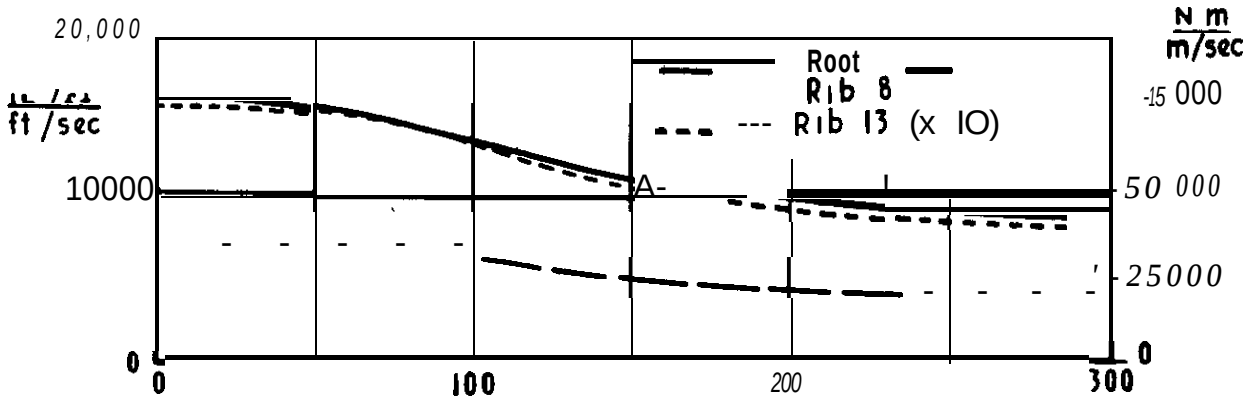

Wing bending moments

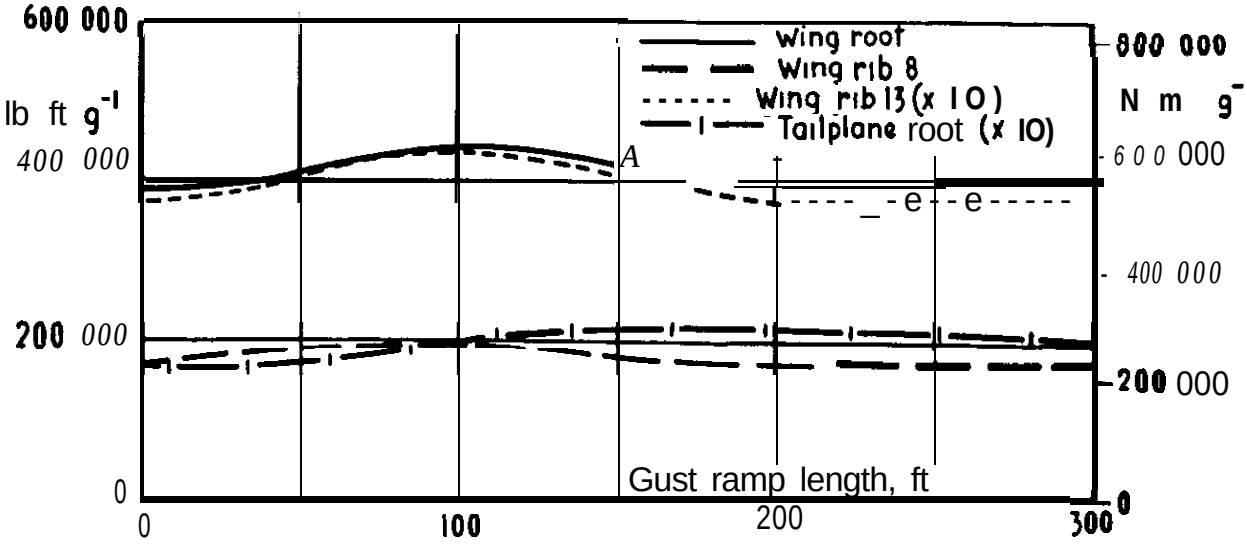

Bending moments per Unit acceleration of the structure near the cg

Fig.13 Variation with gust ramp length of the peak cg acceleration and wing bending moments, and the wing and tailplane bending moments per g

Printed in England for Her Majesty's Stationery Office by the Royal Aircraft Establishment, Farnborough. Dd.135645. K.3

A.R.C. C.P.1035
April 1968

Mitchell, C.O.B.

55X6.013.47 :
629.137.1 :
551.551 :
533.6.048.5

CALCULATION OF THE RESPONSE OF A TRANSPORT AIRCRAFT TO CONTINUOUS TURBULENCE AND DISCRETE GUSTS AND A COMPARISON WITH FLIGHT MEASUREMENTS

me symmetric response of a tri-jet transport aircraft to continuous atmospheric turbulence and to discrete ramp gusts has bee" calculated and compared wlth the results of flight measurements. The aircraft was represented by two rigid and slx elastic modes, and a lifting surface theory was used to calculate airforces. Cockpit and wingtip rms accelerations relative to the cg acceleration were overestimated by the calculations, but wing and tailplane rms bending moments per g agreed with measurements to better than 12% accuracy.

A.R.C. C.P.1035
April 1968

Mitchell, C.G.B.

533.6.013.47 :
629.137.1 :
551.551 :
533.6.048.5

CALCULATION OF THE RESPONSE OF A TRANSPORT AIRCRAFT TO CONTINUOUS TURBULENCE AND DISCRETE GUSTS AND A COMPARISON WITH FLIGHT MEASUREMENTS

me symmetric response of a tri-jet transport aircraft to continuous atmospheric turbulence and to discrete ramp gusts has bean calculated and compared wlth the results 01 flight measurements. The aircraft was represented by two rigid and six elastic ❑ cdes, and a lifting surface theory was used to calculate airforces. Cockpit and wingtip rms accelerations relative to the cg acceleration were overestimated by the calculations, but wing and tailplane rms bending moments per g agreed with measurements to better than 12% accuracy.

A.R.C. C.P.1035
April 1968

Mitchell, C.G.B.

533.6.013.47 :
629.137.1 :
551.551 :
533.6.048.5

CALCULATION OF THE RESPONSE OF A TRANSPORT AIRCRAFT TO CONTINUOUS TURBULENCE AND DISCRETE GUSTS AND A COMPARISON WITH FLIGHT MEASUREMENTS

m a symmetric response 0 1 a tri-jet transport aircraft to continuous atmospheric turbulence and to discrete ramp gusts has been calculated and compared with the results of flight measurements. me aircraft was represented by two rigid and six elastic modes, end a lifting surface theory was used to Calculate airforces. Cockpit and wingtip rms accelerations relative to the cg acceleration were overestimated by the calculations, but wing and tailplane rms bending moments per g agreed with measurements to better than 12% accuracy.

CHAB CARDS

Published by
HER MAJESTY'S STATIONERY OFFICE

To be purchased from
49 High Holborn, London W C.1
13A Castle Street, Edinburgh 2
109 St. Mary Street, Cardiff CF11JW
Brazennose Street, Manchester 2
50 Fairfax Street, Bristol BS13DE
258 Broad Street, Birmingham 1
7 Linenhall street, Belfast BT2 8AY
or through any bookseller

C.P. No. 1035

SBN 11 470162 8